

Supplementary Information of

A novel MOF-808 derived material for oxidative desulfurization: the synergistic effect of hydrophobicity and electron transfer

Chengzhao Zhu¹, Miaomiao Zheng¹, Mingyu Liao¹, Nan Jiang¹, Yuanjie Xiao¹,

Jianbin Liu¹, Linfeng Zhang¹, Jia Guo¹, Huadong Wu^{1,*}, Hao Yan^{2,*}

¹ Key Laboratory of Green Chemical Process of Ministry of Education,
Engineering Research Centre of Phosphorus Resources Development and Utilization
of Ministry of Education, Hubei Key Laboratory of Novel Chemical Reactor and
Green Chemical Technology, Wuhan Institute of Technology, Wuhan 430073, P. R.
China.

² Army Logistics Academy, Chongqing 401331, PR China.

* Corresponding author: Tel: 86-027-87194883;

E-mail address: wuhuadong@wit.edu.cn.

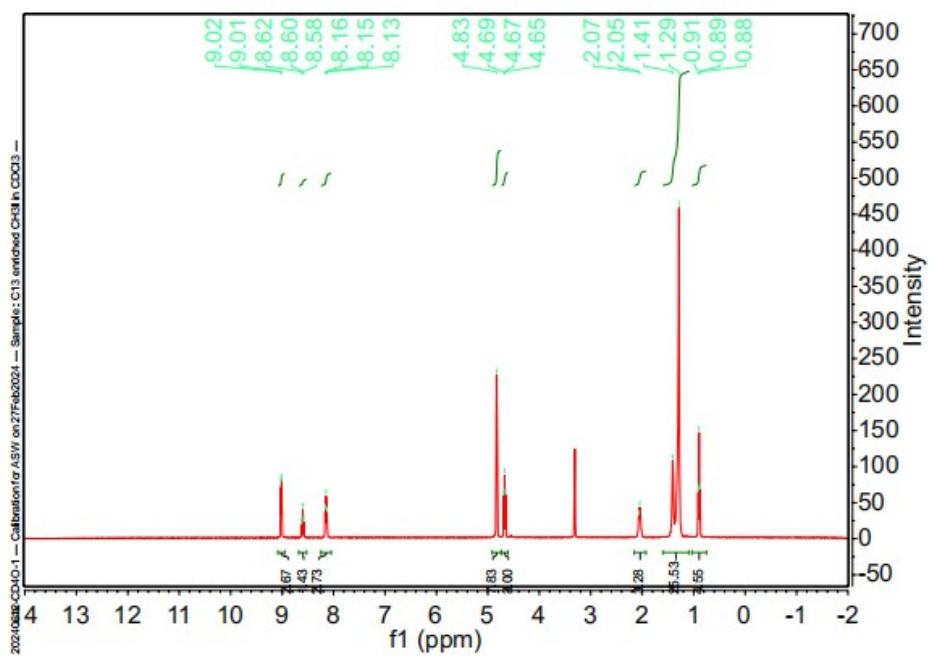


Figure S1. ^1H NMR spectrum of $[\text{C}_{12}\text{Py}]_3(\text{NH}_4)_3\text{Mo}_7\text{O}_{24}$ in CD_4O .

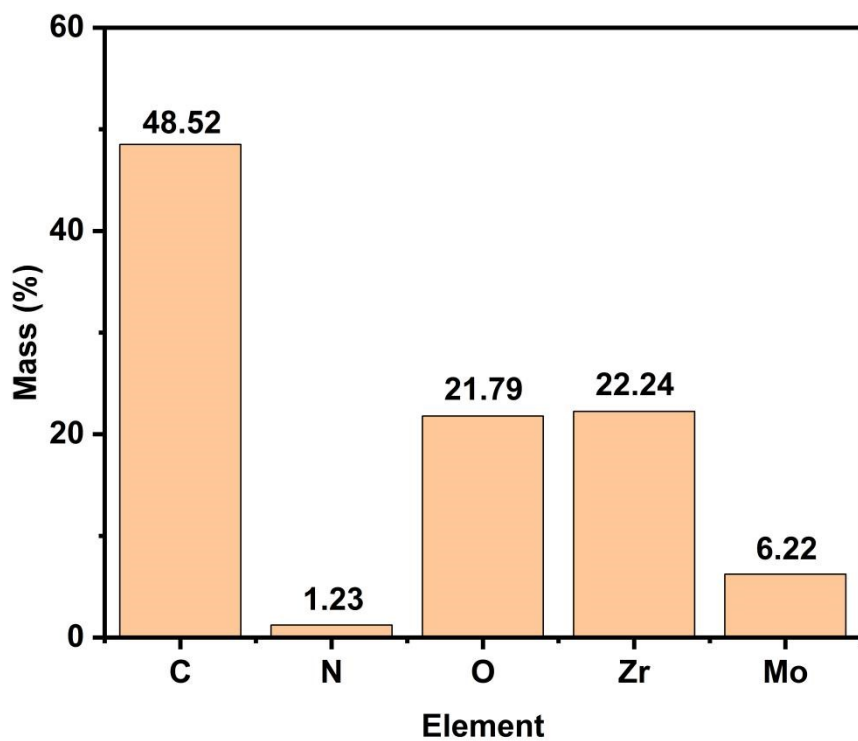


Figure S2. Quality percentage of different elements over $\text{C}_{12}\text{Py}]_3(\text{NH}_4)_3\text{Mo}_7\text{O}_{24}/\text{T-MOF-808-15\%}$.

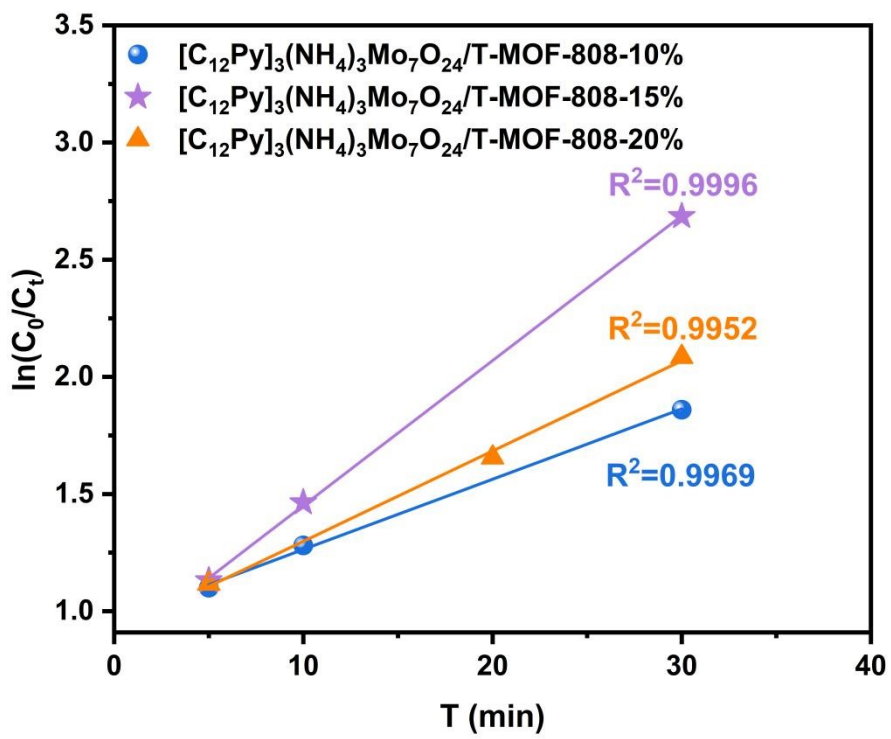


Figure S3. Pseudo-first-order kinetics for the oxidation of DBT at different loading amounts over [C₁₂Py]₃(NH₄)₃Mo₇O₂₄/T-MOF-808.

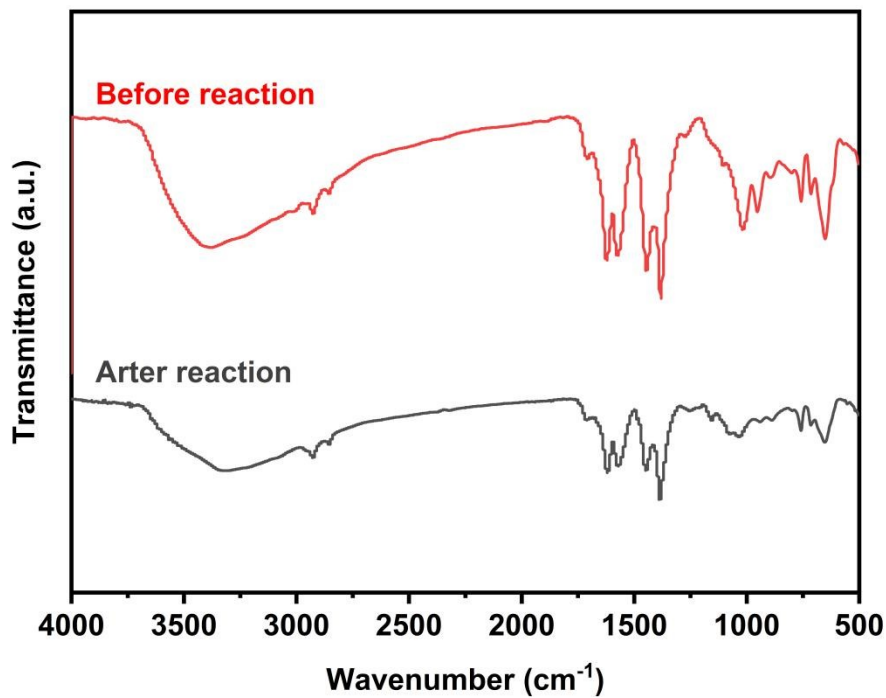


Figure S4. FT-IR spectra of $[C_{12}Py]_3(NH_4)_3Mo_7O_{24}/T\text{-MOF-808-15\%}$ catalyst before and after reaction.

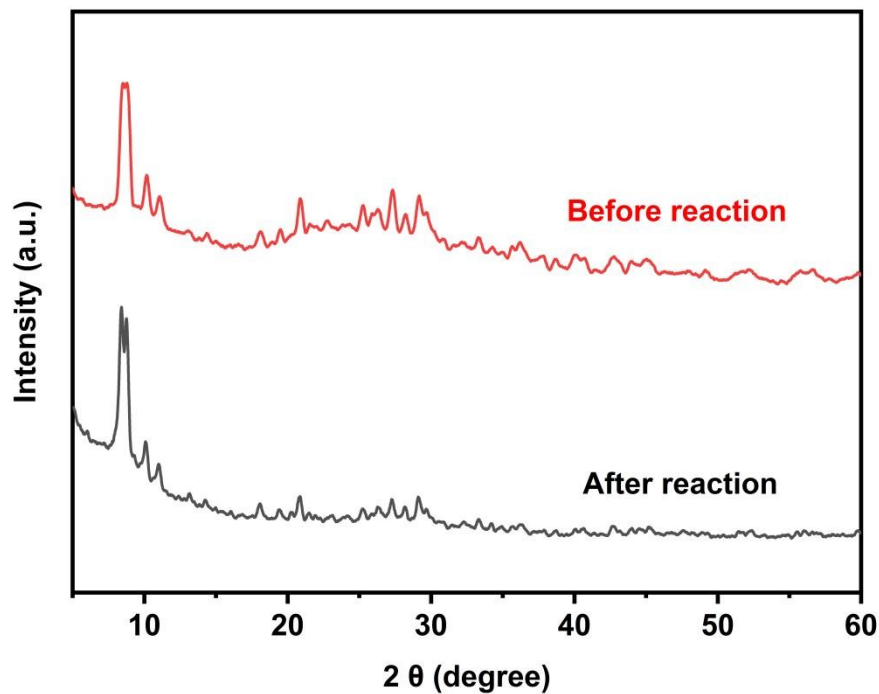


Figure S5. XRD patterns of $[C_{12}Py]_3(NH_4)_3Mo_7O_{24}/T\text{-MOF-808-15\%}$ catalyst before and after reaction.

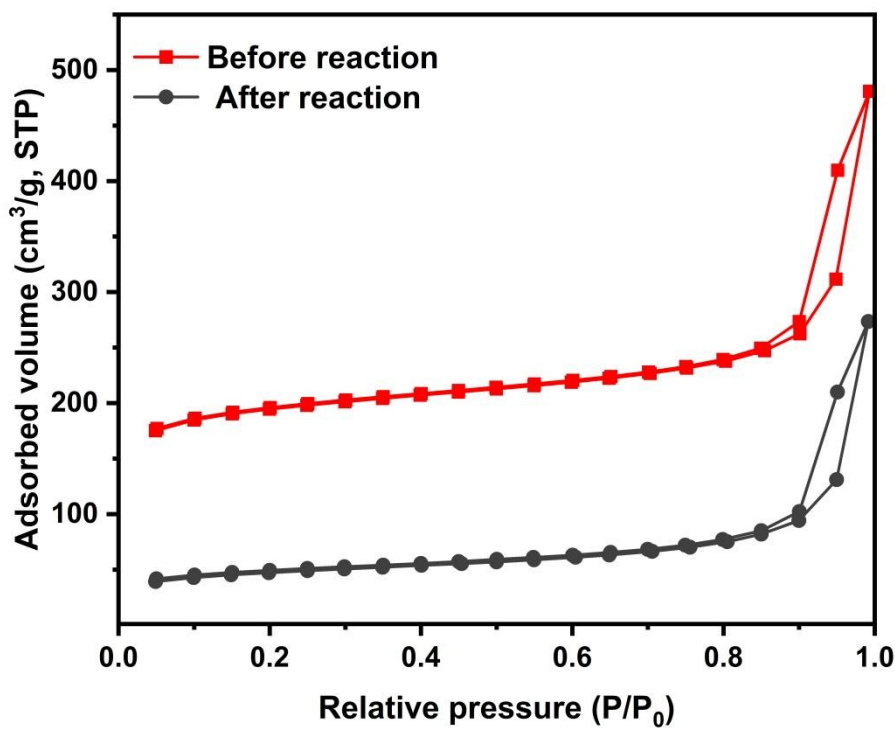


Figure S6. N_2 adsorption-desorption isotherms of $[\text{C}_{12}\text{Py}]_3(\text{NH}_4)_3\text{Mo}_7\text{O}_{24}/\text{T-MOF-808}$ before and after reaction.

Table S1. Textural properties of different samples.

Samples	BET surface area (m ² /g)	Pore Volume (cm ³ /g)	Pore Diameter (nm)
MOF-808	924.78	0.81	3.05
T-MOF-808	899.89	0.74	3.06
[C ₁₂ Py] ₃ (NH ₄) ₃ Mo ₇ O ₂₄ /T-MOF-808-10%	687.21	0.65	17.45
[C ₁₂ Py] ₃ (NH ₄) ₃ Mo ₇ O ₂₄ /T-MOF-808-15%	497.83	0.63	30.99
[C ₁₂ Py] ₃ (NH ₄) ₃ Mo ₇ O ₂₄ /T-MOF-808-20%	205.77	0.31	17.35

Table S2. Reaction rate constant corresponding to different loadings in the ODS reaction.

Load capacity (%)	Rate constant <i>k</i> (min ⁻¹)	Correlation factor R ²
10	0.02999	0.9969
15	0.06185	0.9996
20	0.03851	0.09952

Table S3. Comparison of the ODS performances of different catalysts for DBT

Entry	catalysts	Sulfur ($\mu\text{g}\cdot\text{g}^{-1}$)	Dosage (mg)	T (°C)	O/S	t (min)	Conversi on rate (%)	Ref.
1	UIO-66	500	100	60	12	150	100	[1]
2	PMo ₁₁ /g-C ₃ N ₄	100	100	30	10	20	98.6	[2]
3	UiO-66(Zr)-free	1000	50	60	6	120	99.6	[3]
4	Ti ₃₂ -BTA	200	50	60	6	60	100	[4]
5	PW ₁₂ @TiO ₂	500	85	60	6	60	99.9	[5]
6	[C ₁₂ Py] ₃ (NH ₄) ₃ Mo ₇ O	500	100	60	6	40	100	This work
²⁴ T-MOF-808-15%								

References

- [1] X. Zhang, P. Huang, A. Liu, M. Zhu, A metal–organic framework for oxidative desulfurization: UIO-66(Zr) as a catalyst, *Fuel* 209 (2017) 417-423.
- [2] B. Moeinifard, A. Najafi Chermahini, Mono lacunary phosphomolybdate supported on mesoporous graphitic carbon nitride: An eco-friendly and efficient catalyst for oxidative desulfurization of the model and real fuels, *J. Environ. Chem. Eng.* 9 (4) (2021) 105430.
- [3] G. Ye, D. Zhang, X. Li, K. Leng, W. Zhang, J. Ma, Y. Sun, W. Xu, S. Ma, Boosting Catalytic Performance of Metal–Organic Framework by Increasing the Defects via a Facile and Green Approach, *ACS Appl. Mater. Interfaces* 9 (40) (2017) 34937-34943.
- [4] H.-T. Lv, Y. Cui, G.-D. Zou, N. Li, P. Yang, Y. Fan, Synthesis of titanium-oxo macrocycles and their catalytic properties for oxidative desulfurization, *Dalton Trans.* 48 (37) (2019) 14044-14048.

[5] H. Gao, X. Wu, D. Sun, G. Niu, J. Guan, X. Meng, C. Liu, W. Xia, X. Song, Preparation of core-shell PW12@TiO₂ microspheres and oxidative desulfurization performance, *Dalton Trans.* 48 (17) (2019) 5749-5755.